Journal of Huntington's Disease 13 (2024) 279–299
DOI 10.3233/JHD-240045
IOS Press

Review

Magnetic Resonance Imaging to Detect Structural Brain Changes in Huntington's Disease: A Review of Data from Mouse Models

Jenna Hanrahan[a], Drew P. Locke[a] and Lindsay S. Cahill[a,b,*]
[a]*Department of Chemistry, Memorial University of Newfoundland, St. John's, Newfoundland and Labrador, Canada*
[b]*Discipline of Radiology, Memorial University of Newfoundland, St. John's, Newfoundland and Labrador, Canada*

Accepted 14 July 2024
Pre-press 26 August 2024
Published 10 September 2024

Abstract. Structural magnetic resonance imaging (MRI) is a powerful tool to visualize 3D neuroanatomy and assess pathology and disease progression in neurodegenerative disorders such as Huntington's disease (HD). The development of mouse models of HD that reproduce many of the psychiatric, motor and cognitive impairments observed in human HD has improved our understanding of the disease and provided opportunities for testing novel therapies. Similar to the clinical scenario, MRI of mouse models of HD demonstrates onset and progression of brain pathology. Here, we provided an overview of the articles that used structural MRI in mouse models of HD to date, highlighting the differences between studies and models and describing gaps in the current state of knowledge and recommendations for future studies.

Keywords: Brain structure, Huntington's disease, magnetic resonance imaging, mouse models, neuroanatomy

INTRODUCTION

Huntington's disease (HD) is a neurodegenerative disorder with a known genetic cause.[1] It is autosomal dominant and caused by a CAG repeat expansion in the huntingtin gene (HTT). A CAG repeat length greater than 39 results in full penetrance of the disease and the CAG repeat length is positively correlated with disease severity.[2] HD is characterized by psychiatric disturbances, motor and cognitive impairments and premature death. While clinical diagnosis involves cognitive and motor symptoms and confirmatory genetic testing, structural magnetic resonance imaging (MRI) is often used as a biomarker of disease and to establish disease progression.[3] MRI may also serve as a marker of treatment efficacy.[4] Large human observational studies using structural MRI have revealed that striatal volume loss occurs early in HD (more than 15 years before motor symptoms present),[5–8] with other brain structures, such as the cortex, hippocampus and thalamus, impacted later in disease.[9–12] Clinical findings with respect to white matter volume in HD are more varied but have shown it is also impacted early in disease progression,[6,13]

*Correspondence to: Lindsay S. Cahill, Department of Chemistry, Memorial University of Newfoundland, Arctic Avenue, St John's, NL, Canada A1 C 5S7. Tel.: +1 905 630 8988; E-mail: lcahill@mun.ca.

with the largest changes in the frontal lobe.[8] The rate of brain volume loss has been associated with CAG repeat length.[14,15] At the time of clinical diagnosis, MRI typically reveals large volume loss in the striatum compared to controls (30–52% loss of the caudate, 33–69% loss of the putamen and 37% loss of the nucleus accumbens).[16–18] Preclinical animal models play an important role in studying neurodegenerative diseases like HD. The use of experimental mice allows for genetic manipulation of the HTT gene and invasive experimental assays (e.g., histology, immunohistochemistry), improving our understanding of the mechanisms of HD and providing an avenue to test therapies and potential treatments. Imaging technologies used to study experimental mice are the same as those used clinically. Preclinical MRI systems at high magnetic field strength are often used to study the whole mouse brain as they provide high spatial resolution and good tissue contrast.[19] The high anatomical reproducibility of mouse age-matched wild type brains (~5%) means that small differences in brain structure can be detected in mouse models of disease.[20] The majority of mouse models with a motor or cognitive deficit suggestive of a neurological disease have been shown to have abnormal brain anatomy using MRI[21] and the non-destructive nature of MRI means it can be paired with behavioral testing and biochemical markers post-imaging.

This review intends to provide an overview of the structural brain MRI findings from mouse models of HD. The search for this review was conducted using PubMed and Web of Science databases up to May 2024 using the following search terms: "Huntington", and "Mouse", and "MRI", or "Magnetic Resonance Imaging". Full-length English language peer reviewed, or preprint studies that use structural MRI to study a mouse model of HD were included. Those not using a mouse model of HD ($n = 15$), missing an untreated (e.g., no oral gavage or injections) control group ($n = 19$), or not using structural T1-weighted or T2-weighted anatomical brain MRI ($n = 32$) were excluded.

PRECLINICAL MRI

MRI measures signal emitted from hydrogen atoms (mostly water and fat) after application of a radio-frequency pulse. Spatial localization is achieved using varying magnetic gradients and image contrast depends on the density of hydrogen atoms and the local tissue microenvironment.[22] MRI is often used to study the brain because it is non-invasive and provides excellent contrast between different brain structures. Preclinical MRI of mouse brains has become a powerful tool in biomedical research; however, compared to clinical human MR imaging, the smaller size of the mice presents a challenge. This is addressed with the use of stronger gradients, closer fitting imaging coils, longer scan times and higher magnetic field strengths. An increase in magnetic field strength (measured in Tesla (T)) results in an increase in the signal sensitivity (increased signal-to-noise ratio), allowing for increased image resolution and image fidelity that can be used to detect subtle differences in tissue and physical structure. Imaging at ultrahigh magnetic fields (e.g., 16.4 T) can suffer from susceptibility imaging artifacts (e.g., from the iron in blood and at air-tissue interfaces) and was only used for *ex vivo* imaging in the articles described in this review.

Structural MRI provides information about brain volume on the macroscopic and mesoscopic level. This review excluded studies of brain microstructure that can be imaged in HD mice using MRI approaches such as diffusion tensor imaging.[23–25] All of the structural MRI articles included in this review used anatomical T2-weighted MRI, an imaging method that provides the optimal image contrast between grey matter, white matter and cerebrospinal fluid based on differences in T_2 relaxation times. This high image contrast enables delineation of anatomical brain structures. Structure volumes (in mm^3) can be measured in the brain using manual volumetry, where trained neuroanatomists segment/define specific regions of interest in the brain, or using automated image analysis algorithms that can segment the whole brain into different anatomic regions.

Structural MRI is only one of many techniques used to study and monitor HD clinically. For more information on other MR imaging approaches to study mouse models of HD, we recommend a recent review article.[26] While outside of the scope of this review, it is important to note that several of the 37 articles that met our inclusion criteria also included additional MRI techniques to study other aspects of HD pathology. These included magnetic resonance spectroscopy to measure brain metabolites,[27–31] T2 relaxivity to measure tissue composition,[32–35] diffusion tensor imaging to measure white matter tracts,[31,36,37] functional MRI (fMRI) to measure cerebral blood flow,[38,39] magnetic resonance angiography to visualize vasculature and measure cerebral blood volume,[40] resting state fMRI

to measure brain connectivity,[41] quantitative magnetization transfer for myelin imaging[37] and dynamic contrast enhanced MRI to measure blood-brain barrier permeability.[39,40]

MOUSE MODELS OF HD

There are over 20 different mouse models of HD used in scientific research, with the decision to use a particular model dependent on which aspect of HD you want to model (motor, cognitive, or psychiatric disturbances).[42] The models vary in terms of how they are engineered, the CAG repeat length, and the severity of disease onset/progression. Models can be grouped into 3 categories: N-terminal transgenic, full-length transgenic and full-length knock-in models.[43] N-terminal transgenic animals carry a portion including the CAG repeat region of the 5′ end of the human HTT gene, full-length transgenic models carry the full HTT artificial gene in a yeast or bacterial chromosome, and full-length knock-in models involve the introduction of CAG repeats directly to the mouse Htt gene (Hdh) via recombination. The most studied HD mouse model is the R6/2, an early onset N-terminal transgenic model that has significant striatal atrophy and a shortened lifespan that depends on the CAG repeat length.[44] MRI has been used to study each of the three types of model. The search conducted for this review identified 37 articles from 10 different models of HD that met the inclusion criteria (3 articles include the study of more than one mouse model).

PRECLINICAL STRUCTURAL MRI OF HD MOUSE MODELS

Table 1 summarizes the 37 articles that used structural MRI to study mouse models of HD, including MRI acquisition parameters, data analysis techniques, neuroanatomical changes and correlations between structural MRI and behavioral symptoms or histopathology. The MRI studies aimed to (i) determine differences in brain structure in HD mice compared to controls and/or (ii) track changes in HD neuroanatomy over time. Comparisons between groups were performed using a single imaging time point or multiple time points. There are trade-offs between *in vivo* and *ex vivo* imaging.[20] *In vivo* imaging provides more physiologically relevant experimental conditions and the ability to perform a longitudinal study, while *ex vivo* imaging allows for higher image resolution, elimination of motion artifacts, and the use of non-physiological MR contrast agents. As demonstrated in Zhang et al., it should be noted that there are overall reductions in the total brain volume, irrespective of genotype, after perfusion fixation for *ex vivo* imaging.[45] Of the studies that used a single imaging time point, eight were *in vivo* and six used an *ex vivo* experimental design. To investigate the changes in brain structure over time, the study design can be cross sectional or longitudinal. *In vivo*, longitudinal study designs allow for measurements within the same animal, decreasing the required sample size, while sacrificing the higher image resolution that is possible with an *ex vivo*, cross sectional study. The majority of the MRI articles (21/37, 57%) used *in vivo*, longitudinal MRI to follow the changes in neuroanatomy over the time course of disease. Three of these studies also included an *ex vivo* time point at the end of the longitudinal study, to explore whether higher resolution images revealed any additional neuroanatomical changes. The number of study time points varied significantly from two (e.g., pre-symptomatic to post-symptomatic) up to seven time points. This included seven time points closely spaced to carefully characterize early brain development in the R6/2 mouse model (3–12 weeks of age)[45,46] and seven time points that covered the lifespan of the HdhQ150 mouse model (8–94 weeks of age).[35] In all of the articles, the age of the imaging time points varied substantially, often reflecting the variable disease onset and severity of disease progression in the different mouse models. For example, the imaging time point of 12 weeks of age is pre-symptomatic for the zQ175 and HdhQ250 mouse models and post-symptomatic for the YAC128 and R6/2 mouse models.

Image analysis varied between articles with 19/37 (51%) using manual segmentation of brain structures known to be impacted in human cases of HD (e.g., striatum, cortex, hippocampus). Manual segmentation is time-intensive and limits the number of structures that can be studied. In contrast to using user-defined regions of interest, three morphometry algorithms were used to analyze the brain structures: deformation based morphometry (DBM) (11/37 studies), voxel based morphometry (VBM) (4/37 studies) and tensor based morphometry (TBM) (3/37 studies).[47,48] These automated algorithms provide unbiased, full brain coverage and can be used to determine focal differences in brain structure (voxel-wise) or used in combination with a segmented anatomical atlas to determine structure volume dif-

Table 1
Structural MRI study specifications and results for mouse models of HD

Ref	Mouse Model	Structural MRI Method[a]	Age	Sex	*n*	Analysis technique	Results	Correlation to symptoms or histopathology
Full-length transgenic models								
Jiang, 2011[49]	BACHD	-*In vivo* -T2w -11.7T -0.1 mm^3	60 weeks	M/F	$n = 5$ per group	Manual segmentation (striatum, cortex)	-decrease in striatum and cortex volume	
Aharony, 2015[34]	BACHD	-*In vivo* -T2w -7.0T -0.07 mm^2, 0.8 mm slice thickness	48 weeks	NR	NR	Manual segmentation (striatum, cortex, hippocampus)	-No differences reported	
Mantovani, 2016[50]	BACHD	-*Ex vivo* cross sectional -T2w -16.4 T -Resolution NR	48, 60 weeks	M/F	$n = 6$ per group	Manual segmentation (striatum, cortex, cerebellum)	-No differences reported at either time point	
Lerch, 2008[51]	YAC128	-*Ex vivo* -T2w -7.0T -0.032 mm^3	32 weeks	NR	$n = 9$ per group	Deformation based morphometry (voxel-wise) and striatal volume and shape analysis	-3.4% decrease in striatum volume (left/right asymmetry) -focal decreases in volume in striatum, corpus callosum, olfactory bulb, thalamus, paraflocculus and anterior commissure -focal increases in volume in primary sensorimotor cortex, primary motor cortex, fimbria and parts of the cerebellum	
Lerch, 2008[52]	YAC128	-*Ex vivo* -T2w -7.0T -0.032 mm^3	32 weeks	NR	$n = 9$ per group	Automated segmentation	-increase in cortical thickness in the sensorimotor cortex	
Carroll, 2011[53]	YAC128	-*Ex vivo* cross sectional -T2w -7.0T -0.032 mm^3	4, 12, 32, 48 weeks	M/F	$n = 7$–9 per group	Deformation based morphometry (voxel-wise and structure volumes)	From 12–48 weeks: -3% total brain volume loss -6.5% decrease in absolute striatum volume -decrease in absolute and relative corpus callosum volume At 32 and 48 weeks: -6% increase in relative ventricle volume - increase in relative cerebellum volume - at 48 weeks, thinning in motor cortex -at 48 weeks, 3.5% decrease in relative volume of striatum	

Lewandowski, 2013[38]	YAC128	-*In vivo* longitudinal -T2w -9.4T Resolution NR	20, 32, 44, 56 weeks	M/F	$n = 7–10$ per group	Manual segmentation (striatum)	-decrease in striatum volume only at 44 weeks	
Petrella, 2018[31]	YAC128	-*In vivo* longitudinal -T2w -9.4T -0.0781 mm^2, 0.5 mm slice thickness	12, 24, 36, 48 weeks	M/F	$n = 3–4$ per sex per group	Semi-automated segmentation	From 12–48 weeks: -8.2% decrease in striatum volume -2.1% decrease in hippocampus volume	
N-terminal transgenic								
Rattray, 2013[32]	R6/1	-*In vivo* longitudinal -*Ex vivo* -T2w -7T -*In vivo*: 0.15625 mm^3 -*Ex vivo*: 0.1 mm^2, 0.5 mm slice thickness	*In vivo*: 9, 17 weeks; *Ex vivo*: 19 weeks	M/F	$n = 9–11$ per sex per group	Manual segmentation (whole brain striatum, cortex, hippocampus, corpus callosum) and tensor based morphometry	-total brain volume smaller than controls at both 9 and 17 weeks From 9–17 weeks: -decrease in cortex volume -decrease in hippocampus volume -striatum volume did not decrease over time but was smaller than controls at 17 weeks Compared to controls at 17 weeks: -focal decreases in relative cortex volume and increases in relative posterior ventricular spaces in males but not females Compared to controls at 19 weeks: -focal decreases in cortex volume in both males and females	-no correlation between brain pathology by MRI and behavior testing (rotarod, open field, grip strength, swimming T-maze, fear conditioning, social interaction) -no correlation between brain pathology by MRI and neuronal number
Gatto, 2021[36]	R6/1	-*Ex vivo* cross sectional -T2w -17.6 T -0.2 mm^3	11, 30 weeks	M/F	$n = 4$ per group	Manual segmentation (frontal accessory cortex, cingulate cortex, primary motor cortex, supplementary motor cortex, striatum, hippocampus, corpus callosum)	Compared to controls at 11 weeks: -47.1% decrease in frontal accessory cortex -34.0% decrease in cingulate cortex Compared to controls at 30 weeks: -13.3% decrease in whole brain volume -26.1% decrease in striatum -16.8% decrease in hippocampus -decrease in frontal accessory, cingulate and motor cortices -19.0% decrease in corpus callosum volume -increase in ventricle volume	

(*Continued*)

Table 1
(*Continued*)

Ref	Mouse Model	Structural MRI Method[a]	Age	Sex	*n*	Analysis technique	Results	Correlation to symptoms or histopathology
Casella, 2023[37]	R6/1	-*Ex vivo* -T2w -9.4 T -0.1 mm × 0.1 mm × 0.25 mm	16 weeks	F	*n* = 7–8 per group	Voxel based morphometry	-increase in white matter volume (posterior callosum, external capsule, olfactory bulb)	
Jenkins, 2005[27]	R6/2	-*In vivo* -T2w -4.7T -0.156 mm^2, 1 mm slice thickness	10 weeks	NR	*n* = 6–8 per group	Voxel based morphometry	-12.2% decrease in whole brain -increase in ventricle volume	
Sawiak, 2009[54]	R6/2	-*Ex vivo* -T2w -1.0T -0.070 mm^3	18 weeks	M/F	*n* = 6–7 per sex per group	Manual segmentation (cortex, striatum, amygdala, lateral ventricles and hippocampus)	-decrease in cortex volume -decrease in striatum volume -increase in lateral ventricles and globus pallidus volume	
Sawiak, 2009[55]	R6/2	-*Ex vivo* -T2w -1.0T -0.070 mm^3	18 weeks	M/F	*n* = 13–29 per sex per group	Voxel based morphometry	-focal differences throughout the brain, including the thalamus, hypothalamus, medulla, hippocampus, cortex, amygdala, basal ganglia, and cerebellum -changes in the striatum were heterogeneous	
Zhang, 2010[45]	R6/2	-*In vivo* longitudinal -T2w -*Ex vivo* -*In vivo*: 9.4T -*Ex vivo*: 11.7T -*In vivo*: 0.1 mm × 0.1 mm × 0.25 mm -*Ex vivo*: 0.08 mm^3	*In vivo*: 3,4,5,6,8,10, 12 weeks *Ex vivo*: 12 weeks	M/F	*n* = 7–8 per group	Manual segmentation (striatum, cortex, hippocampus, cerebellum, lateral ventricles)	Compared to controls at 4 weeks (*in vivo*): -decrease in whole brain, striatum, cortex, hippocampus Compared to controls at 12 weeks (*in vivo*): -18.7% decrease in whole brain volume -29.8% decrease in striatum volume -10.6% decrease in cortex volume -31.7% decrease in hippocampus volume -60% increase in ventricle volume Compared to controls at 12 weeks (*ex vivo*): -21.6% decrease in whole brain volume -19.8% decrease of striatum volume -11.8% decrease of cortex -26.6% decrease of hippocampus -347% increase in ventricle volume	-no correlation between rotarod performance (motor function) and cerebellum volume -positive correlation between striatum, cortex, hippocampus and whole brain volumes and rotarod performance

Zacharoff, 2012[28]	R6/2	-*In vivo* longitudinal -T2w -9.4T -0.100 mm^2, 0.3 mm slice thickness	4,8,12,15 weeks	NR	$n = 8$ per group	Manual segmentation (whole brain, cortex, striatum, lateral and third ventricle, hypothalamus, thalamus)	-2.6% decrease per week of striatum volume -2.9% decrease per week of thalamus volume -1.5% decrease per week of hypothalamus volume -1.7% per week decrease of cortex volume -1.6% decrease per week in anterior brain	
Cepeda-Prado, 2012[39]	R6/2	-*In vivo* longitudinal -T2w -9.4T -0.078125 mm^2, 0.6 mm slice thickness	6, 14 weeks	M/F	$n = 5$ per sex per group	Manual segmentation (stria-tum,neocortex, hippocampus, cerebellum, ventricles)	Compared to controls at 14 weeks: -19.9% decrease in striatum volume -19.4% decrease of neocortex volume -16.1% decrease in hippocampus volume	
Aggarwal, 2012[46]	R6/2	-*In vivo* longitudinal -T2w -9.4T - 0.1 mm × 0.1 mm × 0.25 mm	3,4,5,6,8,10,12 weeks	M/F	$n = 7$–8 per group	Deformation based morphometry (voxel-wise)	From 3–5 weeks: -focal decreases in cortex volume From 5–12 weeks: -focal decreases in striatum, thalamus, hippocampus, cortex	
Lin, 2013[40]	R6/2	-*In vivo* longitudinal -T2w -4.7T - 0.039 mm × 0.047 mm × 0.052 mm	5,7,10,12 weeks	NR	$n = 8$ per group	Manual segmentation (striatum, cortex)	From 7–12 weeks: -decrease in striatum volume -decrease in cortex volume -increase in ventricle volume Compared to controls at 12 weeks: -26% decrease in striatum volume -18% decrease in cortex volume	
Rattray, 2013[33]	R6/2	-*In vivo* longitudinal -T2w -7.0T -0.15625 mm^2, 0.5 mm slice thickness	4,8,12,14 weeks	M/F	$n = 9$–11 per sex per group	Manual segmentation (whole brain, cortex, striatum, hippocampus, corpus callosum)	Compared to controls at 8 weeks: -decrease in whole brain volume -decrease in cortex volume -decrease in hippocampus volume only in males -decrease in corpus callosum volume only in males Compared to controls at 12 weeks: -20.5% decrease in striatum volume only for females -decrease in cortex and hippocampus volumes in both sexes -decrease in corpus callosum volume only in males Compared to controls at 14 weeks: -decrease in striatum volume in both females and males -decrease in cortex and hippocampus volumes in both sexes -decrease in corpus callosum volume only in males	-cortical atrophy correlated with decreased rotarod performance (motor function) and lower exploratory behavior in open field -positive correlation between striatum and cortex volumes and neuronal number in males but not in females

(*Continued*)

Table 1
(*Continued*)

Ref	Mouse Model	Structural MRI Method[a]	Age	Sex	*n*	Analysis technique	Results	Correlation to symptoms or histopathology
Sawiak, 2013[56]	R6/2	-*In vivo* -*Ex vivo* -T2w -4.7T -*In vivo*: 0.1 mm^3 -*Ex vivo*: 0.07 mm^3	*In vivo*: 13–16 weeks *Ex vivo*: 18 weeks	M/F	*In vivo*: $n = 6$ per group *Ex vivo*: $n = 42$ per group	Voxel based morphometry	-focal differences in cortex, olfactory bulbs, amygdala, hippocampus	
Sawiak, 2016[57]	R6/2	-*In vivo* longitudinal -T2w -4.7T -0.1 mm^3	250 CAG: 8–21 weeks at 3 week intervals 350 CAG: 8–33 weeks at 3 week intervals	M/F	$n = 25$–35 per group	Tensor based morphometry	-focal decreases in cortex volume in both HD groups, more significantly in 250CAG -increase in ventricle volume in both groups -focal decreases in striatum, hippocampus and cerebellum volumes in both groups	
Teresh-chenko, 2019[58]	R6/2	-*In vivo* -T2w -9.4T - 0.1 mm × 0.1 mm × 0.25 mm	6 weeks	M	$n = 7$–8 per group	Manual segmentation (whole brain, cortex, cerebellum, striatum, globus pallidus, hippocampus, thalamus)	-decrease in whole brain volume -decrease in relative striatum volume -decrease in relative cortex volume	

Cheng, 2011[59]	N171-82Q	-*In vivo* longitudinal -T2w -9.4T -0.1 mm × 0.1 mm × 0.25 mm	6,10,14,18 weeks	M	$n = 10$ per group	Deformation based morphometry (voxel-wise and structure volumes)	Compared to controls at 6 weeks: -12.8% decrease in corpus callosum volume Compared to controls at 10 weeks: -16.6% decrease in amygdala volume -12.5% decrease in hypothalamus -13.8% decrease in thalamus -18.2% decrease in corpus callosum volume -decrease in striatum volume Compared to controls at 14 weeks: -22.5% decrease in amygdala volume -15.2% decrease in hypothalamus -14.1% decrease in thalamus -19.7% decrease in corpus callosum volume -decrease in striatum volume Compared to controls at 18 weeks: -23.7% decrease in amygdala volume -17.4% decrease in hypothalamus -14.7% decrease in thalamus -15.6% decrease in corpus callosum volume -decrease in striatum volume	-positive correlation between striatum and cortex volumes and rotarod performance
Jiang, 2011[49]	N171-82Q	-*In vivo* -T2w -11.7T -0.1 mm^3	16 weeks	M	$n = 5$ per group	Manual segmentation (striatum, cortex)	-decrease in striatum and cortex volume	
Aggarwal, 2012[46]	N171-82Q	-*In vivo* longitudinal -T2w -9.4T - 0.1 mm × 0.1 mm × 0.25 mm	6,10,14 weeks	M	$n = 6$–10 per group	Deformation based morphometry (voxel-wise)	From 6–14 weeks: -focal decreases in cortex, striatum, hippocampus, cortex and amygdala	-positive correlation between volume changes in striatum and cortex and rotarod performance at 14 weeks
Li, 2017[41]	N171-82Q	-*In vivo* -T2w -11.7T -0.104 mm^2, 0.3 mm slice thickness	18 weeks	M	$n = 7$–13 per group	Deformation based morphometry (structure volumes)	-decrease in striatum volume	

(*Continued*)

Table 1
(*Continued*)

Ref	Mouse Model	Structural MRI Method[a]	Age	Sex	*n*	Analysis technique	Results	Correlation to symptoms or histopathology
Knock-in								
Heikkinen, 2012[29]	zQ175	-*In vivo* longitudinal -T2w -7.0 T -0.078125 mm × 0.15625 mm, 0.7 mm slice thickness	12, 16, 32, 48 weeks	F	*n* = 9–10 per group	Manual segmentation (whole brain, striatum, cortex)	From 12–48 weeks in Homozygous zQ175: -11% decrease in whole brain volume -21% decrease in striatum volume -15% decrease in cortex volume From 12–48 weeks in Heterozygous zQ175: -9% decrease in striatum volume -6% decrease in cortex volume	
Peng, 2016[30]	zQ175	-*In vivo* longitudinal -T2w -9.4T - 0.1 mm × 0.1 mm × 0.25 mm	12, 24, 36, 48 weeks	M/F	*n* = 8 per sex per group	Deformation based morphometry (structure volumes)	Compared to controls at each timepoint: -decrease in whole brain volume -decrease in striatum volume -decrease in cortex volume	
Bertoglio, 2018[60]	zQ175	-*In vivo* -T2w -7.0T -0.2 mm × 0.2 mm × 0.25 mm	24 weeks	M	*n* = 18 per group	Manual segmentation (striatum, cerebellum)	-7.7% decrease in relative striatum volume	
Teresh-chenko, 2019[58]	zQ175	-*In vivo* -T2w -9.4T -0.1 mm × 0.1 mm × 0.25 mm	24 weeks	M/F	*n* = 5 per sex per group	Manual segmentation (whole brain, cortex, cerebellum, striatum, globus pallidus, hippocampus, thalamus)	-decrease in whole brain volume -decrease in relative striatum volume -decrease in relative cortex volume -decrease in relative globus pallidus volume -decrease in relative thalamus volume -increase in relative cerebellum volume	

Zhang, 2020[61]	zQ175	-*In vivo* longitudinal -T2w -9.4T -0.1 mm × 0.1 mm × 0.25 mm	3,5,7 weeks	M/F	$n = 6$ per sex per group	Deformation based morphometry (structure volumes)	Compared to controls at 3 weeks: -6.9% increase in striatum volume in males only -10.2% increase in globus pallidus volume in males only Compared to controls at 5 weeks: -4.3% increase in striatum volume in males only -2.9% increase in neocortex volume in males only -3.8% increase in thalamus volume in males only -7.7% increase in nucleus accumbens volume in males only -4.9% increase in cerebellum volume in males only From 5–7 weeks: -decreased striatum volume in males only -decrease in lateral globus pallidus volume in males only -decrease in cerebellum volume in males only
Heikkinen, 2021[62]	zQ175	-*In vivo* longitudinal -T2w -11.7T -0.078 mm^2, 0.45 mm slice thickness	24, 48 weeks	F	$n = 9$ per group	Manual segmentation (whole brain, striatum, cortex)	Compared to controls at 24 and 48 weeks: -decrease in whole brain volume -decrease in striatum volume -decrease in cortex volume
Liu, 2023[63]	zQ175	-*In vivo* longitudinal -T2w -9.4T -0.1 mm × 0.1 mm × 0.25 mm	16,40 weeks	NR	$n = 5$ per group	Deformation based morphometry (structure volumes)	Compared to controls at 40 weeks: -decrease in striatum volume
Auerbach, 2001[64]	HdhQ111 Hdh^{neoQ20}/ $Hdh^{neoQ111}$	-*In vivo* longitudinal -T2w -7.0T -0.78 mm × 0.78 mm × 0.7 mm	8–76 weeks	NR	$n = 12–25$ per group	Manual segmentation (whole brain, ventricles)	-increase in relative ventricle volume
Jin, 2015[65]	HdhQ250	-*In vivo* longitudinal -T2w -9.4T -0.1 mm × 0.1 mm × 0.25 mm	12, 24, 36, 48 weeks	M	$n = 6$ per group	Deformation based morphometry (structure volumes)	Compared to controls at 24 weeks: -4.6% decrease in striatum volume -5.1% decrease in cortex volume

(*Continued*)

Table 1
(*Continued*)

Ref	Mouse Model	Structural MRI Method[a]	Age	Sex	*n*	Analysis technique	Results	Correlation to symptoms or histopathology
Steventon, 2016[66]	HdhQ150	-*In vivo* longitudinal -T2w -*Ex vivo* -9.4T -*In vivo*: 0.120x0.120 mm^2 (slice thickness NR) -*Ex vivo*: 0.060 mm^3	*In vivo*: 28, 76 weeks *Ex vivo*: 80 weeks	M	$n = 25$ per group	Deformation based morphometry (structure volumes) and cortical thickness measurements	Compared to controls at 28 weeks: -5.7% decrease in whole brain volume -decrease in striatum, cortex, thalamus, globus pallidus, hippocampus absolute volumes Compared to controls at 76 weeks: -11.7% decrease in whole brain volume -decrease in striatum, cortex, thalamus, globus pallidus, hippocampus volume -decrease in thickness of the motor cortex	-negative correlation between relative volume change in thalamus and rotarod performance
Teresh-chenko, 2019[58]	HdhQ250	-*In vivo* -T2w -9.4T -0.1 mm × 0.1 mm × 0.25 mm	24 weeks	M/F	$n = 4$–6 per sex per group	Manual segmentation (whole brain, cortex, cerebellum, striatum, globus pallidus, hippocampus)	-decrease in relative striatum volume -decrease in relative cortex volume -increase in relative cerebellum volume	
Rattray, 2017[35]	HdhQ150	-*In vivo* longitudinal -T2w -*Ex vivo* -7.0T -*In vivo*: 0.156 mm^2, 0.5 mm slice thickness -*Ex vivo*: 0.1 mm^2, 0.5 mm slice thickness	8,15,23, 36,52,81, 94 weeks	M/F	$n = 8$–9 per sex per group	Manual segmentation (whole brain, cortex, striatum, hippocampus, corpus callosum) and tensor based morphometry	Males: -from 15 weeks, decrease in whole brain, striatum (26% decrease at 94 weeks) and cortex volume -from 36 weeks, decrease in hippocampus volume - from 81 weeks, decrease in corpus callosum volume Females: -from 8 weeks, decrease in cortex volume -from 23 weeks, decrease in whole brain volume -from 36 weeks, decrease in striatum and hippocampus volume -from 52 weeks, decrease in corpus callosum volume Compared to controls at 94 weeks (*ex vivo*): -focal decrease in thalamus and increase in ventricles	-positive correlation between whole brain, striatum, cortex and hippocampus volumes and grip strength and locomotor activity in open field -positive correlation between striatum volume measured by histology and whole brain and hippocampal volumes by MRI -positive correlation between striatum volume measured by histology and striatum and cortex volumes by MRI for females but not males -no correlations between brain pathology by MRI and neuronal number or neuronal density -no correlations between huntingtin aggregates and MRI brain volumes

Pépin, 2016[67]	Ki140CAG	-*In vivo* -T2w -11.7T -0.07 × 0.07mm^2, 0.3 mm slice thickness	48 weeks	M/F	n = 1–5 per group	Manual segmentation (striatum)	-20.9% decrease in striatum volume
Pérot, 2022[68]	Ki140CAG	-*In vivo* longitudinal -T2w -11.7T -0.1 mm^2, 0.2 mm slice thickness	10, 20, 32, 48, 72 weeks	M	n = 11–12 per group	Deformation based morphometry (structure volumes)	Compared to controls at 72 weeks: -4.3% decrease in striatum volume -5.3% decrease in frontal cortex volume -5.8% decrease in retrosplenial cortex volume -3.3% decrease in motor cortex volume -9.0% increase in ventricle volume

F, female; M, male; n, number of mice; NR, not reported; T, Tesla; T2w, T2-weighted. [a]includes *in vivo*/*ex vivo*, image contrast (T1/T2), longitudinal/cross-sectional, magnetic field strength, image resolution (mm^3 if 3D isotropic, mm^2 if 2D with slice thickness).

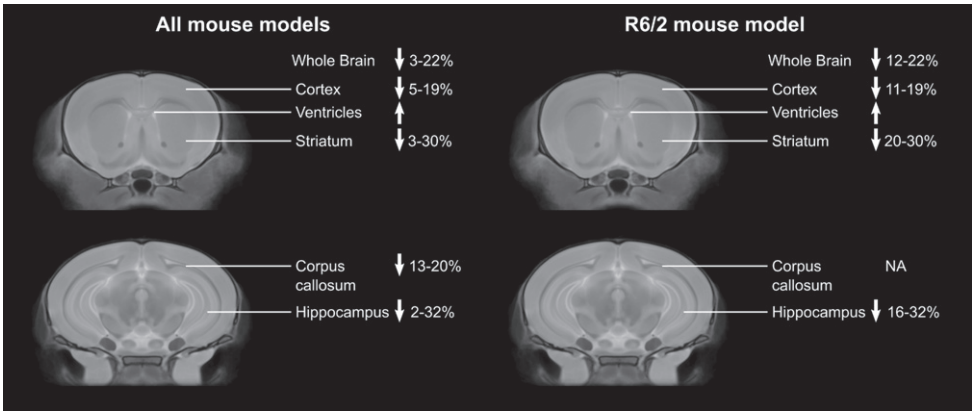

Fig. 1. Percent changes in brain regions compared to controls across studies in all mouse models, and in only the R6/2 mouse model. Only data from articles that provided percent differences or the absolute structure volumes was included.

ferences. Both absolute volumes and relative volumes (normalized to total brain volume to account for variance caused by overall differences in brain volume) were studied.

STRUCTURAL VOLUME CHANGES IN HD MOUSE BRAINS

Figure 1 summarizes the changes in brain structure reported for the 10 different mouse models and the most commonly studied mouse model, the R6/2.

Striatum

Volumetric changes in the striatum of the human brain are a hallmark of HD onset and progression.[69] Structural MRI revealed absolute volume decreases in the striatum in all of the mouse models of HD. These losses ranged from 3–30% across the different models, with the R6/2 mouse model showing the largest decrease compared to controls.[45] Although all of the studies reported decreased striatum volume compared to controls, only 8 of the studies showed progressive striatal atrophy.[28,31,35,40,45,46,57,59] This progression is a human neuroanatomical phenotype of HD[70] and represents an advantage for these models towards clinical translation (YAC128, R6/2, N171-82Q, HdhQ150). In humans, the striatum often undergoes atrophy long before motor and cognitive symptoms occur.[5–8] Most of the mouse studies that included an early imaging time point (before the appearance of overt behavioral phenotypes) did not find significant differences in striatum volume in the HD mice compared to controls.[28,32,33,35,36,39,40,45,46,53,65] With the shortened lifespan of mice compared to humans, this pre-symptomatic atrophy can be challenging to target in the more severe mouse models of HD (e.g., R6/2 mice). Consistent with human HD studies, a decrease in striatum volume was reported in pre-symptomatic N171-82Q[59] and HdhQ150 mice.[66] In male zQ175 mice, Zhang et al reported an increase in striatum volume at 3 weeks, that progressively decreased from 5 to 7 weeks of age.[61]

In addition to investigating total striatum volume, Lerch et al. used striatal shape analysis and reported left-right asymmetry in the striatal atrophy.[51] Several studies using voxel-wise analysis found the volume decreases in the striatum were heterogeneous, with the dorsal, posterior and lateral parts of the striatum being the most affected.[46,51,55]

One advantage of *in vivo*, longitudinal imaging is the ability to explore correlations between structure volume and behavioral outcomes to investigate the neuroanatomical basis of the behavior impairment. While 19 of the mouse MRI studies also included behavioral testing, only seven of the studies examined correlations with neuroanatomical changes. Four of these studies found positive correlations between striatum volume and motor performance (rotarod, locomotor activity in open field test, grip strength).[35,45,46,59]

Cortex

In humans, a decrease in the cortex volume has been reported at different points during clinical presentation in HD.[71] Structural MRI revealed absolute

volume decreases in the cortex in all of the mouse models of HD, ranging from 5–19%. Similar to the striatum, the largest changes were in the R6/2 mouse model.[39] When divided into subcortical regions, large changes were reported for the frontal accessory cortex (47.1%) and the cingulate cortex (34.0%) in R6/1 mice[36] and focal decreases were found in the somatosensory, piriform, motor, frontal, and parietal cortex.[32,46,55–57] Only one article reported increases in cortical regions, with focal increases in the primary sensorimotor and primary motor cortex in YAC128 mice.[51]

Another way to analyze the cortex is by measuring the cortical thickness. Thinning of the cortex, with the sensorimotor cortex most impacted, has been demonstrated in humans with HD.[72] Three mouse MRI studies analyzed the cortical thickness and found it was impacted in HD mice; however, the direction of the effect was inconsistent. Thinning of the motor cortex was found in the HdhQ150[66] and the YAC128 mouse model at 48 weeks of age.[53] In contrast, Lerch et al. demonstrated increased cortical thickness at 32 weeks of age, with the largest difference in the sensorimotor cortex.[52] The difference between the YAC128 studies is that Lerch et al.[52] analyzed the entire cortical thickness while Carroll et al.[53] subdivided the cortex into layers I-V/VI, with the thinning observed only in layers II/III (superficial projection layer) and V/VI (deep projection layers) and a trend towards an increase in layer I. Interestingly, the increased mean cortical thickness at 32 weeks of age correlated to decreased striatal volume, suggesting a potential compensatory response to striatal degeneration.

Compared to the first evidence of striatal atrophy, the majority of mouse studies found the onset of cortical atrophy at a later age. However, two studies in the R6/2 mouse model reported significant decreases in the cortex volume before striatal atrophy was detected.[33,46] Five of the seven studies that explored relationships between neuroanatomy and behavioral changes reported correlations with the cortex volume. The HdhQ150 model exhibited deficits in grip strength which were correlated to the cortical volume decrease.[35] R6/2 and N171-82Q mice showed a correlation between cortex volume and rotarod performance and exploratory behavior.[33,45,46,59]

Hippocampus

In addition to the striatum, the hippocampus is another subcortical region impacted by HD progression.[73] The hippocampus plays a key role in memory and learning, meaning hippocampal atrophy is directly associated with the cognitive impairments observed in HD. Volume changes in the hippocampus were not found in all of the HD mouse models. For example, the mouse MRI studies of the zQ175 and Ki140CAG mice showed sparing of the hippocampus volume. In the YAC128 mouse model, four of the five studies reported no change in the hippocampus volume compared to controls and Petrella et al. only found a small (2.1%) decrease from 12–48 weeks.[31] Moreover, they reported a negative correlation between striatum volume and hippocampus volume, suggesting this correlation reflects an adaptive mechanism. Those studies that did report changes in hippocampus volume ranged from 2–32%, with the largest change in the R6/2 mouse model.[45] This study found a positive correlation between hippocampus volume and rotarod performance.

Thalamus

MRI studies in humans with HD report decreased thalamus volume and associations between thalamic atrophy and cognitive impairments.[74] The majority of the mouse models reported focal and total volume decreases in the thalamus including the YAC128,[51] R6/2,[28,46,55] N171-82Q,[59] zQ175[58,61] and HdhQ150 mice.[35,66] Similar to the striatum volume, the thalamus volume was found to be increased at 3 weeks of age in male zQ175 HD mice and then decreased from 5 to 7 weeks of age.[61] Counterintuitively, a negative correlation between the relative volume change in the thalamus and rotarod performance was reported in the HdhQ150 mouse model.[66]

Cerebellum

Despite the motor impairments associated with human HD, the cerebellum is believed to be spared.[75] The findings with respect to the impact of HD on the cerebellum volume in mouse models were heterogeneous. Cerebellum volume was reported to be increased,[51,53,58,61] decreased,[57] or unchanged.[39,45,46,58,60,65,66] In general, the YAC128 and zQ175 mice appear to have increased cerebellum volume, while the cerebellum is spared in the R6/2 mouse model. Zhang et al. found there was no correlation between motor function (rotarod performance) and cerebellum volume in the R6/2 mouse model.[45]

Ventricles

Ventricle enlargement is a common pathology in human HD.[76] The ventricle volume was shown to be increased compared to controls in YAC128,[53] R6/1,[32,36] R6/2,[27,40,45,54,57] Hdh^{neoQ20}/$Hdh^{neoQ111}$,[64] HdhQ150,[35] and Ki140CAG[68] mouse models. Zhang et al. reported the largest increase, with ventricles 60% larger in R6/2 mice compared to controls at 12 weeks of age.[45] Auerbach et al. found ventricle size was enlarged in only a subset of Hdh^{neoQ20}/$Hdh^{neoQ111}$ mice and that despite worsening phenotype with age, ventricle size did not increase.[64] They conclude that enlarged ventricles are most likely a developmental defect and not a progressive phenotype associated with disease progression.

White matter

The corpus callosum volume decreases in the human brain in HD, resulting in worsening neuropsychological outcomes.[77] Unlike the striatum, cortex and hippocampus, the corpus callosum was not included in all of the studies that performed manual segmentation. Five studies investigated the total volume of the corpus callosum, with four detecting a decrease in the R6/1,[36] R6/2,[33] N171-82Q[59] and HdhQ150 HD mice[35] and one reporting no differences in white matter volume compared to controls in R6/1 mice.[32] The decrease in corpus callosum volume ranged from 13–20% compared to controls. In the R6/2 mice, the decrease in the corpus callosum volume was only detected in males.[33] Focal differences in the corpus callosum were also detected in the YAC128 mice[51,53] and R6/1 mice.[37] The three R6/1 studies provide an illustration of the potential time course of the corpus callosum changes in this mouse model, with an initial localized increase in volume (in the posterior callosum) at 16 weeks of age,[37] followed by no change compared to controls at 17 weeks,[32] and a subsequent decrease in volume of 19% at 30 weeks.[36] In comparison, in the N171-82Q mice, the decrease in corpus callosum volume occurs at the earliest imaging time point (6 weeks of age) and was the only evidence of neuroanatomical atrophy at this age.[59]

Other white matter brain structures that show decreases in HD mice compared to controls include the anterior commissure,[51] external capsule[37] and fimbria.[51]

Other brain structures impacted by HD

46% of the articles used 2D images and manual segmentation of a set of brain structures *expected* to change in HD. As illustrated by the comparison in [54] and [55], 3D, high-resolution isotropic images combined with automated image analysis and VBM (or DBM) finds *new* and *unexpected* (sub)-structures impacted by HD. Other brain structures that were revealed to be impacted by HD include the olfactory bulb,[37,51,56] hypothalamus,[28,55,59] globus pallidus/basal ganglia,[54,55,58,61,66] amygdala[46,55,56,59] and nucleus accumbens.[61]

CAG repeat length

Traditionally, HD severity and the rate of striatal atrophy is associated with CAG repeat length.[2,78] Figure 2 shows the percentage of striatum volume loss measured by structural MRI with CAG repeat length, colored by mouse model. Unlike in human HD, the largest striatal atrophy was observed in mice with the lowest CAG repeat length (at 12 weeks in the R6/2 model[45] and 30 weeks in the R6/1 model).[36] At lower CAG repeat lengths (determined at time of genotyping), there was a U-shaped relationship in striatum volume loss. In Sawiak et al., HD mice with CAG repeat length greater than 200 were described as having an "ameliorated phenotype" compared to mice with fewer repeats.[57] This is consistent with the decrease in the trend line at 200 CAG repeats in Fig. 2 and in the reported delayed disease onset and prolonged survival in other studies of R6/2 mice with > 200 CAG repeats.[79,80,81] It is important to note that striatum volume measurements were taken at different ages and the reported CAG repeat lengths (measured at genotyping) do not account for somatic expansion that occurs with age.[82]

KNOWLEDGE GAPS AND FUTURE DIRECTIONS

1. *Replicability*

   Across all articles there was little replication of results. Study designs (MRI acquisition (e.g., image resolution), sample size, time points, data analysis) varied between all mouse models. Within articles that investigated the same mouse model at the same time point, there is some discrepancy in the structural MRI results. For example, in the YAC128 mouse model, three articles measured striatum volume at 32

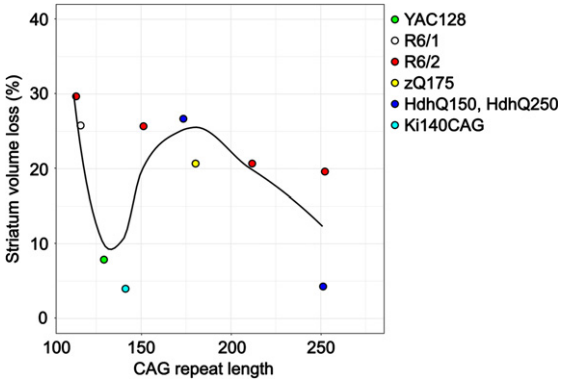

Fig. 2. Striatum volume loss as measured by structural MRI with CAG repeat length in 6 different mouse models. The CAG repeat lengths were determined at the time of genotyping by PCR. Only data from articles that provided percent differences or the absolute structure volumes was included. For mouse models with multiple imaging time points, only data post-symptom onset was included. The average time between motor and cognitive symptom onset and MR imaging was 14 weeks.

weeks of age. However, at this time point, only the two *ex vivo* imaging studies reported a significant decrease in striatum volume,[51,53] while the *in vivo* imaging study reported no significant difference compared to controls.[38] In the zQ175 mouse model, 2 of the 7 articles included a time point at 16 weeks of age. One reported significant decreases in the striatum and cortex volumes at this time point in heterozygous zQ175 mice[29] while another found no changes.[63] The former study had a larger sample size ($n = 9$–10 in Heikkinen et al.[29] vs. $n = 5$ in Liu et al.[63]) which may explain the ability to detect significant volume differences (on the order of 4–8%). Four of the articles about zQ175 mice included a time point at 24 weeks of age and the use of relative brain structure volumes (normalized to total brain volume) in Tereshchenko et al.[58] resulted in the identification of a larger number of structures impacted by HD compared to the three other studies that only looked at absolute structure volumes.[30,60,62] Of the 12 articles that used structural MRI in R6/2 mice, the time points ranged from 3 to 21 weeks of age. Two articles used the same imaging data; however, the analysis approach was different. In Zhang et al., manual segmentation found significant differences at 4 weeks of age in the striatum, cortex, and hippocampus.[45] In contrast, deformation based morphometry from 3–5 weeks of age only showed focal decreases in the cortex.[46] In other studies where there was overlap at the 4 week time point, there were no significant volume differences reported.[28,33] These inconsistencies may be attributed to differences in image resolution, sample size or CAG repeat length. These examples illustrate the impact of study design on MRI outcomes and lack of replicability represents a significant challenge in determining which mouse model best reproduces clinical HD pathology. We recommend following the guidelines in Lerch et al.[20] for experimental design and comparing the different HD mouse models including the use of voxel-wise and both absolute and relative structure volumes, well-powered sample sizes and an appropriate number of time points to explore the full disease progression (including early life, as described below). We also recommend making the structural MRI images freely available to other researchers using a repository such as the Cambridge MRI database.[83]

2. *Early life imaging*

One of the limitations of the use of HD mouse models is that the shortened lifespan means the brain atrophy observed in humans is not fully recapitulated. For example, at clinical diagnosis, the striatum volume in humans is decreased by 30–69%.[17,18] In comparison, the largest striatum volume loss observed in mice was 30%.[45] In the HD mouse models with a more severe phenotype, it is challenging to separate out the impact of the mutation on brain development versus HD pathology. The striatum in the R6/2 mouse model is shown to be different from controls at the earliest imaging time point (3 weeks of age),[61] suggesting the differences are programmed early in life. Moreover, one of the studies of the R6/2 model found there was no progression in the striatal atrophy as the pathological burden increased,[33] indicating it is unaffected by the onset of pathology. This has been observed in the TgCRND8 mouse model of Alzheimer's disease,[84] where abnormal neuroanatomy compared to controls was observed at 1 week of age (before amyloid plaque deposition). Interestingly, a growing body of literature suggests mutant HTT has an impact on brain development, supporting the idea that abnormal neurodevelopment is part of the pathology of HD.[85] Children at risk of HD (CAG repeat length > 39) show striatum volume changes very similar to the R6/2 mice in Zhang et al.[61]: an early increase relative to

controls, followed by a significant progressive decrease.[86] MR imaging of HD mouse models in early life is important to better understand the impact of the HD mutation throughout the lifespan. Mice can be imaged as early as postnatal day 1,[87] providing valuable information about whether the mutation causes a neurodevelopmental phenotype in addition to modeling HD pathology.

3. *Biological sex differences*

   Another important consideration for future studies is understanding sex as a biological variable in HD. Recent human studies have reported significant sex differences in motor, cognitive and depressive symptoms in people with HD.[88] Several of the mouse MRI articles only included one sex and while many used both female and male mice, they were underpowered for exploring sex differences and did not include sex as a biological variable in the data analysis. The MRI mouse studies that did explore sex differences generally found an earlier and more severe impact of HD in males. In R6/1, focal decreases in the cortex volume were observed in males at 17 weeks of age and in females only starting at 19 weeks.[32] In R6/2 mice, males showed a decrease in hippocampus and corpus callosum volumes at 8 weeks of age while atrophy to the hippocampus was not apparent in females until 12 weeks and there was no significant differences between female R6/2 mice and controls in the corpus callosum volume up to 14 weeks.[33] However, striatum volume was significantly decreased in R6/2 females and not in males at 12 weeks of age.[33] In the study of early brain development in zQ175 mice, only males showed volumetric differences compared to controls.[61] Finally, there were significant sex differences in HdhQ150 mice, with females showing cortical atrophy before males and males showing a greater decrease in striatum volume at 95 weeks compared to females.[35] These results support the recommendation that both sexes must be included in the study design and that biological sex must be included in the data analysis.

4. *Other animal models of HD*

   Large animal models of HD provide several unique advantages compared to mice (reviewed recently in Howland et al.).[89] While the majority of MRI studies of HD have been conducted in mouse models, a structural MRI study in transgenic HD non-human primates reported decreased striatum volume and increased lateral ventricle volume, consistent with human HD.[90] Diffusion tensor MR imaging has been conducted in the OVT73 sheep model of HD[91] and the feasibility of using structural MRI in a minipig model of HD has been demonstrated.[92] Future MRI research of both small and large animals promises to bridge the gap between preclinical studies and human HD.

CONCLUSIONS

HD is associated with brain atrophy and structural MRI plays an important role as a clinical biomarker of disease progression. Mouse models of HD provide an avenue for improving our understanding of human disease and for testing novel therapies. Several studies have used structural MRI to investigate treatment efficacy on HD mouse models.[93–97] In order to evaluate these therapies, we need to know how the brain pathology develops over time in each untreated mouse model. Compared to histological assessments, MRI provides a non-invasive, three-dimensional, whole brain approach to image the HD brain and an opportunity to correlate the structure volumes with behavioral outcomes. Mouse models of HD show variable disease progression and pathology and therefore it is not surprising that the MRI-detectable neuroanatomical changes are also variable. When deciding on which mouse model to use, it is important to consider which neuroanatomical aspect and which time point in development is desired. Taken together, the MRI mouse studies reviewed in this paper provides a detailed picture of the time course of neuroanatomical changes that occur in some of the most widely used mouse models of HD.

ACKNOWLEDGMENTS

The authors have no acknowledgments to report.

FUNDING

The funding for this work was provided by Brain Canada. JH and DPL acknowledge financial support from CIHR and NSERC, respectively.

CONFLICT OF INTEREST

The authors have no conflict of interest to report.

REFERENCES

1. Parsons MP and Raymond LA. Huntington disease. In: Zigmond MJ, Wiley CA and Chesselet M-F (eds) *Neurobiology of Brain Disorders*. 2nd ed. Academic Press, 2023, pp. 275–292.
2. Langbehn DR, Registry Investigators of the European Huntington Disease Network. Longer CAG repeat length is associated with shorter survival after disease onset in Huntington disease. *Am J Hum Genet* 2022; 109: 172–179.
3. Ross CA, Aylward EH, Wild EJ, et al. Huntington disease: Natural history, biomarkers, and prospects for therapeutics. *Nat Rev Neurol* 2014; 10: 204–216.
4. Wijeratne PA, Johnson EB, Gregory S, et al. A multi-study model-based evaluation of the sequence of imaging and clinical biomarker change in Huntington's disease. *Front Big Data* 2021; 4: 662200.
5. Paulsen JS, Long JD, Ross CA, et al. Prediction of manifest Huntington's disease with clinical and imaging measures: A prospective observational study. *Lancet Neurol* 2014; 13: 1193–1201.
6. Tabrizi SJ, Scahill RI, Owen G, et al. Predictors of phenotypic progression and disease onset in premanifest and early-stage Huntington's disease in the TRACK-HD study: Analysis of 36-month observational data. *Lancet Neurol* 2013; 12: 637–649.
7. Domínguez JF, Stout JC, Poudel G, et al. Multimodal imaging biomarkers in premanifest and early Huntington's disease: 30-month IMAGE-HD data. *Br J Psychiatry* 2016; 208: 571–578.
8. Aylward EH, Nopoulos PC, Ross CA, et al. Longitudinal change in regional brain volumes in prodromal Huntington disease. *J Neurol Neurosurg Psychiatry* 2011; 82: 405–410.
9. Bates GP, Dorsey R, Gusella JF, et al. Huntington disease. *Nat Rev Dis Primers* 2015; 1: 15005.
10. Georgiou-Karistianis N, Scahill R, Tabrizi SJ, et al. Structural MRI in Huntington's disease and recommendations for its potential use in clinical trials. *Neurosci Biobehav Rev* 2013; 37: 480–490.
11. McColgan P and Tabrizi SJ. Huntington's disease: A clinical review. *Eur J Neurol* 2018; 25: 24–34.
12. Scahill RI, Andre R, Tabrizi SJ, et al. Structural imaging in premanifest and manifest Huntington disease. *Handb Clin Neurol* 2017; 144: 247–261.
13. Gregory S, Johnson E, Byrne LM, et al. Characterizing white matter in Huntington's disease. *Mov Disord Clin Pract* 2020; 7: 52–60.
14. Ruocco HH, Bonilha L, Li LM, et al. Longitudinal analysis of regional grey matter loss in Huntington disease: Effects of the length of the expanded CAG repeat length. *J Neurol Neurosurg Psychiatry* 2008; 79: 130–135.
15. Langbehn DR, Stout JC, Gregory S, et al. Association of CAG repeats with long-term progression in Huntington disease. *JAMA Neurol* 2019; 76: 1375–1385.
16. Kinnunen KM, Schwarz AJ, Turner EC, et al. Volumetric MRI-based biomarkers in Huntington's Disease: An evidentiary review. *Front Neurol* 2021; 12: 712555.
17. van den Bogaard SJ, Dumas EM, Acharya TP, et al. Early atrophy of pallidum and accumbens nucleus in Huntington's disease. *J Neurol* 2011; 258: 412–420.
18. Aylward EH, Sparks BF, Field KM, et al. Onset and rate of striatal atrophy in preclinical Huntington disease. *Neurology* 2004; 63: 66–72.
19. Henkelman RM. Systems biology through mouse imaging centers: Experience and new directions. *Annu Rev Biomed Eng* 2010; 12: 143–166.
20. Lerch JP, Gazdzinski L, Germann J, et al. Wanted dead or alive? The tradeoff between in-vivo versus ex-vivo MR brain imaging in the mouse. *Front Neuroinform* 2012; 6: 6.
21. Nieman BJ, Lerch JP, Bock NA, et al. Mouse behavioral mutants have neuroimaging abnormalities. *Hum Brain Mapp* 2007; 28: 567–575.
22. Plewes DB and Kucharczyk W. Physics of MRI: A primer. *J Magn Reson Imaging* 2012; 35: 1038–1054.
23. Vorisek I, Syka M and Vargova L. Brain diffusivity and structural changes in the R6/2 mouse model of Huntington disease. *J Neurosci Res* 2017; 95: 1474–1484.
24. Gatto RG, Ye AQ, Colon-Perez L, et al. Detection of axonal degeneration in a mouse model of Huntington's disease: Comparison between diffusion tensor imaging and anomalous diffusion metrics. *Magn Reson Mater Phys* 2019; 32: 461–471.
25. Gatto RG and Weissmann C. Preliminary examination of early neuroconnectivity features in the R6/1 mouse model of Huntington's disease by ultra-high field diffusion MRI. *Neural Regen Res* 2022; 17: 983–986.
26. Pérot J-B, Brouillet E and Flament J. The contribution of preclinical magnetic resonance imaging and spectroscopy to Huntington's disease. *Front Aging Neurosci* 2024; 16: 1306312.
27. Jenkins BG, Andreassen OA, Dedeoglu A, et al. Effects of CAG repeat length, HTT protein length and protein context on cerebral metabolism measured using magnetic resonance spectroscopy in transgenic mouse models of Huntington's disease. *J Neurochem* 2005; 95: 553–562.
28. Zacharoff L, Tkac I, Song Q, et al. Cortical metabolites as biomarkers in the R6/2 model of Huntington's disease. *J Cereb Blood Flow Metab* 2012; 32: 502–514.
29. Heikkinen T, Lehtimäki K, Vartiainen N, et al. Characterization of neurophysiological and behavioral changes, MRI brain volumetry and 1H MRS in zQ175 knock-in mouse model of Huntington's disease. *PLoS One* 2012; 7: e50717.
30. Peng Q, Wu B, Jiang M, et al. Characterization of behavioral, neuropathological brain metabolic and key molecular changes in zQ175 knock-in mouse model of Huntington's disease. *PLoS One* 2016; 11: e0148839.
31. Petrella LI, Castelhano JM, Ribeiro M, et al. A whole brain longitudinal study in the YAC128 mouse model of Huntington's disease shows distinct trajectories of neurochemical, structural connectivity and volumetric changes. *Hum Mol Genet* 2018; 27: 2125–2137.
32. Rattray I, Smith EJ, Crum WR, et al. Correlations of behavioral deficits with brain pathology assessed through longitudinal MRI and histopathology in the R6/1 mouse model of Huntington's disease. *PLoS One* 2013; 8: e84726.
33. Rattray I, Smith E, Gale R, et al. Correlations of behavioral deficits with brain pathology assessed through longitudinal MRI and histopathology in the R6/2 mouse model of HD. *PLoS One* 2013; 8: e60012.
34. Aharony I, Ehrnhoefer DE, Shruster A, et al. A Huntingtin-based peptide inhibitor of caspase-6 provides protection from

mutant Huntingtin-induced motor or behavioral deficits. *Hum Mol Genet* 2015; 24: 2604–2614.
35. Rattray I, Smith EJ, Crum WR, et al. Correlations of behavioral deficits with brain pathology assessed through longitudinal MRI and histopathology in the HdhQ150/Q150 mouse model of Huntington's disease. *PLoS One* 2017; 12: e0168556.
36. Gatto RG, Weissmann C, Amin M, et al. Evaluation of early microstructural changes in the R6/1 mouse model of Huntington's disease by ultra-high field diffusion MR imaging. *Neurobiol Aging* 2021; 102: 32–49.
37. Casella C, Kelly B, Murillo Bartolome A, et al. Differences in white matter detected by *ex vivo* 9.4T MRI are associated with axonal changes in the R6/1 model of Huntington's disease. *bioRxiv* 2023; doi: 10.1101/2023.10.02.560424 [Preprint]. Posted October 02, 2023.
38. Lewandowski NM, Bordelon Y, Brickman AM, et al. Regional vulnerability in Huntington's disease: fMRI-guided molecular analysis in patients and a mouse model of disease. *Neurobiol Dis* 2013; 52: 84–93.
39. Cepeda-Prado E, Popp S, Khan U, et al. R6/2 Huntington's disease mice develop early and progressive abnormal brain metabolism and seizures. *J Neurosci* 2012; 32: 6456–6467.
40. Lin C-Y, Hsu Y-H, Lin M-H, et al. Neurovascular abnormalities in humans and mice with Huntington's disease. *Exp Neurol* 2013; 250: 20–30.
41. Li Q, Li G, Wu D, et al. Resting-state functional MRI reveals altered brain connectivity and its correlation with motor dysfunction in a mouse model of Huntington's disease. *Sci Rep* 2017; 7: 16742.
42. Pouladi MA, Morton AJ, Hayden MR. Choosing an animal model for the study of Huntington's disease. *Nat Rev Neurosci* 2013; 14: 708–721.
43. Menalled L, Lutz C, Ramboz S, et al. A field guide to working with mouse models of Huntington's disease. https://chdifoundation.org/wp-content/uploads/HD_Field_Guide_040414.pdf (2014, accessed 10 June 2024).
44. Mangiarini L, Sathasivam K, Seller M, et al. Exon 1 of the HD gene with an expanded CAG repeat is sufficient to cause a progressive neurological phenotype in transgenic mice. *Cell* 1996; 87: 493–506.
45. Zhang J, Peng Q, Li Q, et al. Longitudinal characterization of brain atrophy of a Huntington's disease mouse model by automated morphological analyses of magnetic resonance images. *Neuroimage* 2010; 49: 2340–2351.
46. Aggarwal M, Duan W, Hou Z, et al. Spatiotemporal mapping of brain atrophy in mouse models of Huntington's disease using longitudinal *in vivo* magnetic resonance imaging. *Neuroimage* 2015; 60: 2086–2095.
47. Chung MK, Worsley KJ, Paus T, et al. A unified statistical approach to deformation-based morphometry. *Neuroimage* 2001; 14: 595–606.
48. Ashburner J and Friston KJ. Voxel-based morphometry – the methods. *Neuroimage* 2000; 11: 805–821.
49. Jiang M, Wang J, Fu J, et al. Neuroprotective role of Sirt1 in mammalian models of Huntington's disease through activation of multiple Sirt1 targets. *Nat Med* 2011; 18: 153–158.
50. Mantovani S, Gordon R, Li R, et al. Motor deficits associated with Huntington's disease occur in the absence of striatal degradation in BACHD transgenic mice. *Hum Mol Genet* 2016; 25: 1780–1791.
51. Lerch JP, Carroll JB, Spring S, et al. Automated deformation analysis in the YAC128 Huntington disease mouse model. *Neuroimage* 2008; 39: 32–39.
52. Lerch JP, Carroll JB, Dorr A, et al. Cortical thickness measured from MRI in the YAC128 mouse model of Huntington's disease. *Neuroimage* 2008; 41: 243–251.
53. Carroll JB, Lerch JP, Franciosi S, et al. Natural history of disease in the YAC128 mouse reveals a discrete signature of pathology in Huntington disease. *Neurobiol Dis* 2011; 43: 257–265.
54. Sawiak SJ, Wood NI, Williams GB, et al. Use of magnetic resonance imaging for anatomical phenotyping of the R6/2 mouse model of Huntington's disease. *Neurobiol Dis* 2009; 33: 12–19.
55. Sawiak SJ, Wood NI, Williams GB, et al. Voxel-based morphometry in the R6/2 transgenic mouse reveals differences between genotypes not seen with manual 2D morphometry. *Neurobiol Dis* 2009; 33: 20–27.
56. Sawiak SJ, Wood NI, Williams GB, et al. Voxel-based morphometry with templates and validation in a mouse model of Huntington's disease. *Magn Reson Imaging* 2013; 31: 1522–1531.
57. Sawiak SJ, Wood NI and Morton AJ. Similar progression of morphological and metabolic phenotype in R6/2 mice with different CAG repeats revealed by *in vivo* magnetic resonance imaging and spectroscopy. *J Huntingtons Dis* 2016; 5: 271–283.
58. Tereshchenko A, Magnotta V, Epping E, et al. Brain structure in juvenile-onset Huntington disease. *Neurology* 2019; 92: e1939–e1947.
59. Cheng Y, Peng Q, Hou Z, et al. Structural MRI detects progressive regional brain atrophy and neuroprotective effects in N171-82Q Huntington's disease mouse model. *Neuroimage* 2011; 56: 1027–1034.
60. Bertoglio D, Verhaeghe J, Kosten L, et al. MR-based spatial normalization improves [18F]MNI-659 PET regional quantification and detectability of disease effect in the Q175 mouse model of Huntington's disease. *PLoS One* 2018; 13: e0206613.
61. Zhang C, Wu Q, Liu H, et al. Abnormal brain development in Huntington' disease is recapitulated in the zQ175 knock-in mouse model. *Cereb Cortex Commun* 2020; 1: tgaa044.
62. Heikkinen T, Bragge T, Kuosmanen J, et al. Global Rhes knockout in the Q175 Huntington's disease mouse model. *PLoS One* 2021; 16: e0258486.
63. Liu H, Chen L, Zhang C, et al. Interrogation of dynamic glucose-enhanced MRI and fluorescence-based imaging reveals a perturbed glymphatic network in Huntington's disease. *bioRxiv* 2023; doi: 10.1101/2023.04.03.535397 [Preprint]. Posted April 03, 2023.
64. Auerbach W, Hurlbert MS, Hilditch-Maguire P, et al. The HD mutation causes progressive lethal neurological disease in mice expressing reduced levels of huntingtin. *Hum Mol Genet* 2001; 10: 2515–2523.
65. Jin J, Peng Q, Hou Z, et al. Early white matter abnormalities, progressive brain pathology and motor deficits in a novel knock-in mouse model of Huntington's disease. *Hum Mol Genet* 2015; 24: 2508–2527.
66. Steventon JJ, Trueman RC, Ma D, et al. Longitudinal *in vivo* MRI in a Huntington's disease mouse model: Global atrophy in the absence of white matter microstructural damage. *Sci Rep* 2016; 1: 32423.
67. Pépin J, Francelle L, Carrillo-de Sauvage MA, et al. *In vivo* imaging of brain glutamate defects in a knock-in mouse model of Huntington's disease. *Neuroimage* 2016; 1: 53–64.
68. Pérot J-B, Célestine M, Palombo M, et al. Longitudinal multimodal MRI characterization of a knock-in mouse model

of Huntington's disease reveals early gray and white matter alterations. *Hum Mol Genet* 2022; 31: 3581–3596.
69. Harris GJ, Pearlson GD, Peyser CE, et al. Putamen volume reduction on magnetic resonance imaging exceeds caudate changes in mild Huntington's disease. *Ann Neurol* 1992; 31: 69–75.
70. Rosas HD, Goodman J, Chen YI, et al. Striatal volume loss in HD as measured by MRI and the influence of CAG repeat. *Neurology* 2001; 57: 1025–1028.
71. Halliday GM, McRitchie DA, Macdonald V, et al. Regional specificity of brain atrophy in Huntington's disease. *Exp Neurol* 1998; 154: 663–672.
72. Rosas HD, Liu AK, Hersch S, et al. Regional and progressive thinning of the cortical ribbon in Huntington's disease. *Neurology* 2002; 58: 695–701.
73. Wilkes FA, Jakabek D, Walterfang M, et al. Hippocampal morphology in Huntington's disease, implications for plasticity and pathogenesis: The IMAGE-HD study. *Psychiatry Res Neuroimaging* 2023; 335: 111694.
74. Kassubek J, Juengling FD, Ecker D, et al. Thalamic atrophy in Huntington's disease co-varies with cognitive performance: A morphometric MRI analysis. *Cereb Cortex* 2005; 15: 846–853.
75. Paulsen JS, Nopoulos PC, Aylward E, et al. Striatal and white matter predictors of estimated diagnosis for Huntington disease. *Brain Res Bull* 2010; 82: 201–207.
76. Hobbs NZ, Barnes J, Frost C, et al. Onset and progression of pathologic atrophy in Huntington disease: A longitudinal MR imaging study. *AJNR Am J Neuroradiol* 2010; 31: 1036–1041.
77. Estevez-Fraga C, Scahill R, Rees G, et al. Diffusion imaging in Huntington's disease: A comprehensive review. *J Neurol Neurosurg Psychiatry* 2020; 92: 62–69.
78. Aylward E, Mills J, Liu D, et al. Association between age and striatal volume stratified by CAG repeat length in prodromal Huntington disease. *PLoS Curr* 2011; 3: RRN1235.
79. Morton AJ, Glynn D, Leavens W, et al. Paradoxical delay in the onset of disease caused by super-long CAG repeat expansions in R6/2 mice. *Neurobiol Dis* 2009; 33: 331–341.
80. Dragatsis I, Goldowitz D, Del Mar N, et al. CAG repeat lengths > or = 335 attenuate the phenotype in the R6/2 Huntington's disease transgenic mouse. *Neurobiol Dis* 2008; 33: 315–330.
81. Cummings DM, Alaghband Y, Hickey MA, et al. A critical window of CAG repeat-length correlates with phenotype severity in the R6/2 mouse model of Huntington's disease. *J Neurophysiol* 2012; 107: 677–691.
82. Mangiarini L, Sathasivam K, Mahal A, et al. Instability of highly expanded CAG repeats in mice transgenic for the Huntington's disease mutation. *Nat Genet* 1997; 15: 197–200.
83. Sawiak SJ and Morton AJ. The Cambridge MRI database for animal models of Huntington disease. *Neuroimage* 2016; 124: 1260–1262.
84. Grand-Allemang R, Scholz J, Ellegood J, et al. Altered brain development in an early-onset murine model of Alzheimer's disease. *Neurobiol Aging* 2015; 36: 638–647.
85. van der Plas E, Schultz JL and Nopoulos PC. The neurodevelopmental Hypothesis of Huntington's disease. *J Huntingtons Dis* 2020; 9: 217–229.
86. van der Plas E, Langbehn DR, Conrad AL, et al. Abnormal brain development in child adolescent carriers of mutant huntingtin. *Neurology* 2019; 93: e1021–e1030.
87. Szulc KU, Lerch JP, Nieman BJ, et al. 4D MEMRI atlas of neonatal FVB/N mouse brain development. *Neuroimage* 2015; 118: 49–62.
88. Hentosh S, Zhu L, Patino J, et al. Sex differences in Huntington's disease: Evaluating the Enroll-HD database. *Mov Disord Clin Pract* 2021; 8: 420–426.
89. Howland D, Ellederova Z, Aronin N, et al. Large animal models of Huntington's disease: What we have learned and where we need to go next. *J Huntingtons Dis* 2020; 9: 201–216.
90. Chan AWS, Jiang J, Chen Y, et al. Progressive cognitive deficit, motor impairment and striatal pathology in a transgenic Huntington disease monkey model from infancy to childhood. *PLoS One* 2015; 10: e0122335.
91. Taghian T, Gallagher J, Batcho E, et al. Brain alterations in aged OVT73 sheep model of Huntington's disease: An MRI based approach. *J Huntingtons Dis* 2022; 11: 391–406.
92. Schubert R, Frank F, Nagelmann N, et al. Neuroimaging of a minipig model of Huntington's disease: Feasibility of volumetric, diffusion-weighted and spectroscopic assessments. *J Neurosci Methods* 2016; 265: 46–55.
93. Lee JH, Sowada MJ, Boudreau RL, et al. Rhes suppression enhances disease phenotypes in Huntington's disease mice. *J Huntingtons Dis* 2014; 3: 65–71.
94. Wang S-E, Lin C-L, Hsu C-H, et al. Treatment with a herbal formula B401 enhances neuroprotection and angiogenesis in the R6/2 mouse model of Huntington's disease. *Drug Des Devel Ther* 2015; 16: 887–900.
95. Garcia-Miralles M, Hong X, Juin Tan L, et al. Laquinimod rescues striatal, cortical and white matter pathology and results in modest behavioural improvements in the YAC128 model of Huntington disease. *Sci Rep* 2016; 16: 31652.
96. Zhou X, Li G, Kaplan A, et al. Small molecule modulator of protein disulfide isomerase attenuates mutant huntingtin toxicity and inhibits endoplasmic reticulum stress in a mouse model of Huntington's disease. *Hum Mol Genet* 2018; 27: 1545–1555.
97. Simmons DA, Mills BD, Butler RR, et al. Neuroimaging, urinary, and plasma biomarkers of treatment response in Huntington's disease: Preclinical evidence with the $p75^{NTR}$ ligand LM11A-31. *Neurotherapeutics* 2021; 18: 1039–1063.